J|A|C|S
ARTICLES
Published on Web 02/09/2006

Formation and Dissociation of Intra−Intermolecular Hydrogen-Bonded Solute−Solvent Complexes: Chemical Exchange Two-Dimensional Infrared Vibrational Echo Spectroscopy

Junrong Zheng, Kyungwon Kwak, Xin Chen, John B. Asbury,† and M. D. Fayer*

Contribution from the Department of Chemistry, Stanford University, Stanford, California 94305

Received October 17, 2005; E-mail: fayer@stanford.edu

Abstract: 2-Methoxyphenol (2MP) solutes form weak complexes with toluene solvent molecules. The complexes are unusual in that the 2MP hydroxyl has an intramolecular hydrogen bond and simultaneously forms an intermolecular hydrogen bond with toluene and other aromatic solvents. In the equilibrated solute−solvent solution, there exists approximately the same concentration of 2MP−toluene complex and free 2MP. The very fast formation and dissociation (chemical exchange) of this type of three-centered hydrogen bond complex were observed in real time under thermal equilibrium conditions with two-dimensional (2D) infrared vibrational echo spectroscopy. Chemical exchange is manifested in the 2D spectrum by the growth of off-diagonal peaks. Both the formation and dissociation can be characterized in terms of the dissociation time constant, which was determined to be 3 ps for the 2MP−toluene complex. The intra−intermolecular hydrogen bond formation is influenced by subtle details of the molecular structure. Although 2MP forms a complex with toluene, it is demonstrated that 2-ethoxyphenol (2EP) does not form complexes to any significant extent. Density functional calculations at the B3LYP/6-31+G(d,p) level suggest that steric effects caused by the extra methyl group in 2EP are responsible for the difference.

I. Introduction

Hydrogen bonding is ubiquitous in nature. It is involved in the most basic and important chemical and biological phenomena.[1−3] The strength of hydrogen bonds lies between van der Waals forces and covalent bonds. Although not a true chemical bond, a hydrogen bond is sufficiently strong and directional to become the driving force for molecules to assemble into delicate architectures in supramolecular chemistry, molecular recognition, and self-assembly. The strength of hydrogen bonds is in the range of energies that permits rapid association and dissociation under ambient conditions. Such rapid hydrogen bond dynamics are important in a wide variety of systems, such as the properties of water[4] and biological recognition.[3] Hydrogen bonding has been studied extensively in many contexts since the birth of the concept in the early 1900s.[2,3,5]

Hydrogen bonds can be separated into two categories: intermolecular hydrogen bonds in which the hydrogen bond donor and acceptor are in different molecules and intramolecular hydrogen bonds in which the donor and acceptor are in the same molecule.[5] In general, intramolecular hydrogen bonds form five-, six-, or seven-membered rings,[2] where the geometric restrictions make them relatively weak compared to intermolecular hydrogen bonds involving the same type of donor and acceptor. Because of geometrical constraints, intramolecular hydrogen bonds cannot form with the optimal geometry compared to the intermolecular ones, creating the possibility that the donor of an intramolecular hydrogen bond can form an additional intermolecular hydrogen bond with an appropriate acceptor located on another molecule. A special type of hydrogen bond will form under these conditions. This type of hydrogen bond involves three centers, one donor, and two acceptors. There is another type of three-centered hydrogen bond with one acceptor and two donors, which is common when the acceptor has two electron lone pairs; e.g., in a molecule such as water, the oxygen can be the acceptor for two hydrogen donors on two other water molecules. The "intra−intermolecular hydrogen bond" discussed above has a single donor with two acceptors. This type of three-centered hydrogen bond, which is also called "bifurcated",[6] plays important roles in many chemical and biological systems, e.g., chiral molecular recognition,[7] proteins,[8] RNA,[9] DNA,[10] and carbohydrates.[11] Kinetic studies of the formation and dissociation

† Permanent address: Department of Chemistry, Penn State University, University Park, PA 16802.

(1) Pimentel, G. C.; McClellan, A. L. *Annu. Rev. Phys. Chem.* **1971**, *22*, 347−385.
(2) Pimentel, G. C.; McClellan, A. L. *The Hydrogen Bond*; W. H. Freeman and Co.: San Francisco, 1960.
(3) Desiraju, G. R.; Steiner, T. *The Weak Hydrogen Bond*; Oxford: New York, 1999.
(4) Bertolini, D.; Cassettari, M.; Ferrario, M.; Grigolini, P.; Salvetti, G. *Adv. Chem. Phys.* **1985**, *62*, 277−320.
(5) Jeffrey, G. A. *An Introduction to Hydrogen Bonding*; Oxford University Press: New York, 1997.
(6) Steiner, T. *Angew. Chem., Int. Ed.* **2002**, *41*, 48−76.
(7) Kim, S.-G.; Kim, K.-H.; Kim, Y. K.; Shin, S. K.; Ahn, K. H. *J. Am. Chem. Soc.* **2003**, *125*, 13819−13824.
(8) Sundaralingam, M.; Sekharudu, Y. C. *Science* **1989**, *244*, 1333−1337.
(9) Auffinger, P.; Westhol, E. *J. Mol. Biol.* **1999**, *292*, 467−483.
(10) Nelson, H. C. M.; Finch, J. T.; Luisi, B. F.; Klug, A. *Nature* **1987**, *330*, 221−226.

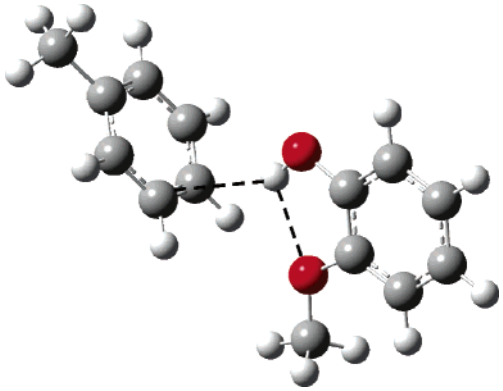

Figure 1. Structure of the intra−intermolecular hydrogen-bonded complex of 2-methoxyphenol and toluene in the isolated state calculated with DFT at the B3LYP/6-31+G(d,p) level.

of this type of hydrogen bond in liquid solutions are challenging because of its ultrafast time scale.

As described in detail below, 2-methoxyphenol (2MP) is an example of intra−intermolecular hydrogen bonding when it is dissolved in toluene or other aromatic solvents. 2MP forms an intramolecular hydrogen bond with the oxygen on the methoxyl group, the acceptor for the hydroxyl hydrogen donor. The formation enthalpy of the intramolecular hydrogen bond of 2MP in cyclohexane was determined to be −2.0 kcal/mol on the basis of the spectroscopic data.[12] When 2MP is dissolved in toluene, an intra−intermolecular hydrogen bond is formed, in which the π-electrons of the benzene ring act as a weak hydrogen bond acceptor. The formation enthalpy of the intermolecular part of this three-centered hydrogen bond was determined to be ∼−0.6 kcal/mol (see below). The calculated structure of the 2MP−toluene complex is shown in Figure 1. The calculation was done with density functional theory (DFT) at the B3LYP/6-31+G-(d,p) level. The calculation is for the isolated molecules; that is, there is no solvent in the calculation. The distance between the hydrogen atom and the intramolecular acceptor oxygen is ∼2.18 Å, whereas for the pure intramolecular hydrogen bond, the distance is ∼2.11 Å. The distance change shows that the intramolecular interaction is weakened by the intermolecular interaction. The 2MP hydroxyl hydrogen atom points roughly to the center of one of the C−C bonds that is para to the methyl group of the toluene. The distance between the 2MP hydrogen atom and the toluene *meta*-carbon atom is ∼2.74 Å, and the distance to the *para*-carbon is ∼2.82 Å.

In the following, linear spectroscopic evidence will be presented for the existence of the complex shown in Figure 1 and for the formation enthalpy of the intra−intermolecular hydrogen bond. Then, ultrafast two-dimensional (2D) IR vibrational echo spectroscopy (2D IR VES) is used to measure the dynamics of chemical exchange between the 2MP−toluene complex and free 2MP in a solution of low concentration of 2MP and toluene as the solvent and to support the species assignments made by linear spectroscopy. The formation and dissociation of the three-centered hydrogen bond are directly monitored by observing the growth of off-diagonal peaks in the 2D IR vibrational echo spectrum. [13−15] The measurements provide the fast dynamics of solute−solvent complex formation and dissociation under thermal equilibrium conditions, as has recently been demonstrated for a different type of solute−solvent complex system.[13,14] Another 2D IR technique, narrow bandwidth pump/broad bandwidth probe, has been used to study chemical exchange.[16] The 2D IR VES method is a Fourier transform spectroscopy like Fourier transform NMR and Fourier transform IR, which can frequently provide superior data when compared to non-Fourier transform methods. The observation of fast chemical exchange processes[14,15] is another advance in 2D IR VES. 2D IR VES has been developed and applied to a variety of problems over the last several years.[17−26]

II. Experimental Procedures

The 2D IR VES experimental setup is similar to that described previously.[27] Briefly, three successive IR pulses (∼1 μJ/pulse) with the same polarization were applied to induce the subsequent emission in a distinct direction of a time-delayed 4th pulse, the vibrational echo. The transform-limited pulses (∼50 fs, ∼4 cycles of light) are produced using a Ti/Sapphire regeneratively amplified laser system pumping an optical parametric amplifier. The IR pulses span sufficient bandwidth (300 cm^{-1} centered at ∼4 μm or 2500 cm^{-1}) to cover the $v = 0$ to $v = 1$ transition (denoted 0−1) and the $v = 1$ to $v = 2$ transition (denoted 1−2) of the hydroxyl OD stretching modes in both intramolecular and intra−intermolecular hydrogen-bonded 2MPOD. The OD hydroxyl stretch was studied rather than OH because the 2500 cm^{-1} frequency region associated with the OD stretch has less overlap with other modes. The vibrational echo pulse is detected with frequency and phase resolution by combining it with a 5th (local oscillator) pulse, and the combined pulses are dispersed in a spectrograph. The function of the local oscillator is to phase resolve and amplify the vibrational echo signal. Data are thus obtained as a function of three variables: the emitted vibrational echo frequencies ω_m and the variable time delays between the first and second pulses (τ) and the second and third pulses (T_w, the variable "waiting" time). By numerical Fourier transform (FT), the τ scan data taken at every ω_m are mapped to a second frequency variable ω_τ for each T_w. The data are then plotted in three dimensions, the amplitude as a function of both ω_τ and ω_m, which correspond to the ω_1 and ω_3 axes, respectively, in 2D NMR. The 2D vibrational echo spectra presented here are obtained with the dual scan technique[27−30]

(11) Taylor, R.; Kennard, O.; Versichel, W. *J. Am. Chem. Soc.* **1984**, *106*, 244−248.
(12) Carlson, G. L.; Fateley, W. G. *J. Phys. Chem.* **1973**, *77*, 1157−1163.
(13) Fayer, M. D.; Zheng, J.; Kwak, K.; Asbury, J. B. In *Molecular Dynamics/Theoretical Chemistry Meeting*, Monterey, California, May 22−24, 2005; Berman, M., Ed.
(14) Zheng, J.; Kwak, K.; Asbury, J. B.; Chen, X.; Piletic, I.; Fayer, M. D. *Science* **2005**, *309*, 1338−1343.
(15) Kim, Y. S.; Hochstrasser, R. M. *Proc. Natl. Acad. Sci. U.S.A.* **2005**, *102*, 11185−11190.
(16) Woutersen, S.; Mu, Y.; Stock, G.; Hamm, P. *Chem. Phys.* **2001**, *266*, 137−147.
(17) Zanni, M. T.; Hochstrasser, R. M. *Curr. Opin. Struct. Biol.* **2001**, *11*, 516−522.
(18) Golonzka, O.; Khalil, M.; Demirdoven, N.; Tokmakoff, A. *Phys. Rev. Lett.* **2001**, *86*, 2154−2157.
(19) Merchant, K. A.; Thompson, D. E.; Fayer, M. D. *Phys. Rev. Lett.* **2001**, *86*, 3899−3902.
(20) Volkov, V.; Schanz, R.; Hamm, P. *Opt. Lett.* **2005**, *30*, 2010−2012.
(21) Zanni, M. T.; Gnanakaran, S.; Stenger, J.; Hochstrasser, R. M. *J. Phys. Chem. B* **2001**, *105*, 6520−6535.
(22) Asbury, J. B.; Steinel, T.; Stromberg, C.; Gaffney, K. J.; Piletic, I. R.; Goun, A.; Fayer, M. D. *Phys. Rev. Lett.* **2003**, *91*, 237402.
(23) Steinel, T.; Asbury, J. B.; Corcelli, S. A.; Lawrence, C. P.; Skinner, J. L.; Fayer, M. D. *Chem. Phys. Lett.* **2004**, *386*, 295−300.
(24) Asbury, J. B.; Steinel, T.; Fayer, M. D. *Chem. Phys. Lett.* **2003**, *381*, 139−146.
(25) Zheng, J.; Kwak, K.; Steinel, T.; Asbury, J. B.; Chen, X.; Xie, J.; Fayer, M. D. *J. Chem. Phys.* **2005**, *123*, 164301.
(26) Khalil, M.; Demirdoven, N.; Tokmakoff, A. *J. Phys. Chem. A.* **2003**, *107*, 5258−5279.
(27) Asbury, J. B.; Steinel, T.; Fayer, M. D. *J. Lumin.* **2004**, *107*, 217−286.
(28) Khalil, M.; Demirdoven, N.; Tokmakoff, A. *Phys. Rev. Lett.* **2003**, *90*, 047401 (047404).
(29) Asbury, J. B.; Steinel, T.; Stromberg, C.; Gaffney, K. J.; Piletic, I. R.; Fayer, M. D. *J. Chem. Phys.* **2003**, *119*, 12981−12997.
(30) Asbury, J. B.; Steinel, T.; Stromberg, C.; Gaffney, K. J.; Piletic, I. R.; Goun, A.; Fayer, M. D. *Chem. Phys. Lett.* **2003**, *374*, 362−371.

to reduce or eliminate dispersive contributions to the spectra. The phase correction procedure followed the method described previously.[27] The samples for the vibrational echo experiments are 3 wt % 2MPOD (OD = hydroxyl OH replaced by OD), *p*-methyl-*o*-methoxylphenolOD (pMMPOD), and 2-exothyphenolOD (2EPOD) in toluene between 3-mm thick CaF_2 windows with a 0.2-mm Teflon spacer.

The OD stretch vibrational lifetimes and rotational relaxation times for the samples were measured with the polarization selective IR pump−probe experiments. The polarization selective IR pump−probe experimental setup is similar to one described previously.[31] The laser source is the same as that used for the vibrational echo experiments. For the pump−probe experiments, the mid-IR pulse was spitted into two beams of intensity ratio 20:1. The beam with higher intensity served as the pump. The weaker one was the probe beam. The pump beam had horizontal polarization, and the probe beam polarization was 45° relative to the pump beam. The probe beam was passed through a spectrograph and detected by a 32-element MCT array detector. A polarizer was placed in front of the monochromator aligned to selectively measure the parallel or perpendicular polarized signal relative to the pump beam. Because the orientational relaxation is relatively fast compared to the vibrational lifetime, it was possible to tail match the signals for the two polarizations to eliminate possible errors introduced by differences in the amplitudes of the signals for the two polarizations. The method eliminates possible sources of error such as phase shifts caused by mirrors and different diffraction efficiencies of the grating for different polarizations.[32] The sample concentrations and cells are the same as those used in the vibrational echo experiments.

Because the intramolecular and intra−intermolecular hydrogen-bonded 2MPODs in toluene exchange on the same time scale as the OD stretch vibrational and rotational decays, the vibrational lifetimes and rational relaxation constants for the species cannot be obtained directly by performing pump−probe experiments on the 2MPOD/toluene solution. The vibrational lifetime for the intramolecular hydrogen-bonded 2MPOD in toluene was obtained by performing experiments on 2EPOD/toluene solution because 2EPOD does not form a complex with toluene, as discussed in detail below. It is assumed that the addition of one methyl will not make a significant change in the vibrational lifetime as it is well removed from the OD. The rotational relaxation time constant for the intramolecular hydrogen-bonded 2MP was obtained by correcting the measured value for the 2EPOD by the small volume difference between 2MPOD and 2EPOD. The rotational relaxation constant for the intra−intermolecular hydrogen-bonded 2MP in toluene was obtained by measuring that of *p*-methoxyphenolOD (pMPOD) in toluene solution. pMPOD forms a much stronger complex than 2MPOD because of the lack of the intramolecular hydrogen bond. In toluene, there are essentially only pMPOD−toluene complexes, and therefore, the complex orientational relaxation time can be measured. The OD stretch lifetime of the intra−intermolecular bonded 2MPOD was determined using the method described in Section III. B.

The formation enthalpy of the intermolecular part of the intra−intermolecular hydrogen bonding for 2MPOD in toluene was obtained by performing temperature-dependent FTIR measurements on the 3 wt % 2MPOD in toluene solution. The same sample cells as those used in the vibrational echo experiments were used. The equilibrium constant for the two species in the 2MPOD/toluene solution was obtained by comparing the areas of each peak obtained by fitting the FTIR spectrum to Gaussian line shapes and correcting for the difference in extinction coefficients. The extinction coefficient ratio for the intramolecular and intra−intermolecular hydrogen-bonded 2MPOD in toluene was obtained by comparing the 2D and one-dimensional (1D) IR results. The volume of each peak at a very short T_w in a 2D IR spectrum is proportional to the product of the concentration and the 4th power of the transition dipole moment of the species.[33] The area of each peak in a 1D IR spectrum is proportional to the product of the concentration and the extinction coefficient (the square of the transition dipole moment) of each species.[34] Dividing the volume from the 2D IR spectrum at T_w = 200 fs by the area from the 1D IR spectrum for the same species from the same sample determined the extinction coefficient ratio for the intra−intermolecular to the intramolecular hydrogen-bonded 2MPOD to be 2.0.

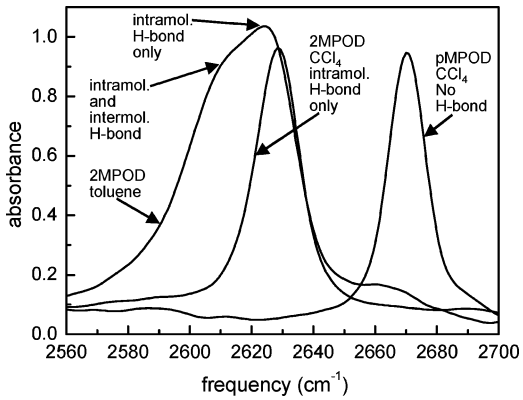

Figure 2. FTIR spectra of 0.25 wt % *p*-methoxyphenolOD in CCl_4, 1.3 wt % 2-methoxyphenolOD in CCl_4, and 2 wt % 2-methoxyphenolOD in toluene, showing the non-hydrogen-bonded, intramolecular hydrogen-bonded, and intra−intermolecular hydrogen-bonded OD stretch peaks, respectively.

All chemicals were purchased from Aldrich. They were used as received. The deuterated hydroxyl hydrogen (OD) of the phenol derivatives was prepared by deuterium exchange with methanolOD. To obtain the deuterated phenol derivatives, 1 g of each undeuterated phenol derivative was dissolved in 10 g of methanolOD and stirred for 0.5 h. The solvent was then removed under vacuum. The procedure was repeated three times, and compounds with >90% deuteration of the hydroxyl hydrogen were obtained.

The electronic structure calculations were carried out using density functional theory,[35] as implemented in the Gaussian 98 program suite. The level and basis set used were Becke's three-parameter hybrid functional combined with the Lee−Yang−Parr correction functional, abbreviated as B3LYP and 6-31+G(d,p). All results reported here do not include the surrounding solvent and therefore are for the isolated molecules.

III. Results and Discussions

A. Linear Spectroscopy. The experimental evidence for the non-hydrogen-bonded, intramolecular hydrogen-bonded, and intra−intermolecular hydrogen-bonded species is shown in Figure 2. FTIR spectra in Figure 2 are for 0.25 wt % pMPOD in CCl_4, 1.3 wt % 2MPOD in CCl_4, and 2 wt % 2MPOD in toluene. The peak at 2670 cm^{-1} is for the free OD stretch. In CCl_4, phenol does not form an intermolecular complex when the concentration is low enough to avoid phenol oligomers.[1,14] A para-substituted phenol has chemical properties similar to those for an ortho-substituted one, so the non-hydrogen-bonded OD stretch of the pMPOD will have essentially the same frequency as 2MPOD would have if it did not form an intramolecular hydrogen bond. Therefore, the spectrum of pMPOD displays the OD stretch in the absence of both

(31) Tan, H.-S.; Piletic, I. R.; Fayer, M. D. *J. Chem. Phys.* **2005**, *122*, 174501 (174509).
(32) Tan, H.-S.; Piletic, I. R.; Fayer, M. D. *J. Opt. Soc. Am. B* **2005**, *22*, 2009−2017.
(33) Mukamel, S. *Principles of Nonlinear Optical Spectroscopy*; Oxford University Press: New York, 1995.
(34) Fayer, M. D. *Elements of Quantum Mechanics*; Oxford University Press: New York, 2001.
(35) Parr, R. G.; Yang, W. *Density Functional Theory of Atoms and Molecules*; Oxford University Press: New York, 1989.

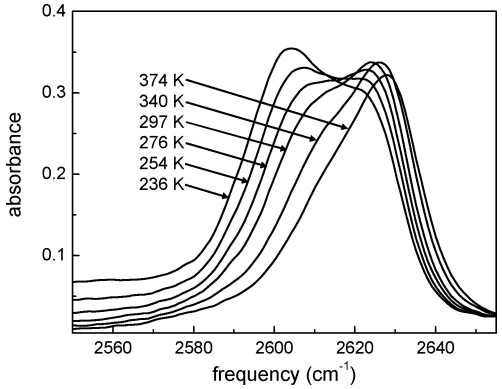

Figure 3. Temperature-dependent FTIR spectra of 3 wt % 2-methoxyphenolOD in toluene from 236 to 374 K.

intermolecular and intramolecular hydrogen bonding. The 2MPOD spectrum in CCl_4 displays the spectrum of the intramolecular hydrogen-bonded OD stretch at 2629 cm^{-1}. The hydrogen bond produces a shift to lower frequency (red shift).[2] The spectrum for 2MPOD in toluene is considerably broader than the spectrum in CCl_4. The spectrum consists of one main peak and an approximately equal amplitude shoulder. The main peak has the same frequency as the peak in CCl_4. Therefore, we attribute it to the intramolecular hydrogen-bonded OD stretch in the absence of the intermolecular complex formation (free 2MPOD). The shoulder at around 2611 cm^{-1} arises from the intra−intermolecular hydrogen-bonded OD stretch, which is further red shifted because of the additional hydrogen bonding. Both the intramolecular hydrogen-bonded and intra−intermolecular hydrogen-bonded 2MP are prominent in the toluene solution because the formation Gibbs free energy of the intermolecular part of the intra−intermolecular hydrogen bond is very small (see below). It was found that the frequency change for the hydrogen-bonded hydroxyl stretch is linearly proportional to the formation enthalpy of the hydrogen bond for the same donor.[1] Our results are consistent with this observation. Additional FTIR experiments and the 2D IR VES data presented below confirm the identification of the main peak and the shoulder as the free 2MPOD and the 2MPOD−toluene complex, respectively.

Figure 3 is the temperature-dependent FTIR spectra of the 2MPOD in toluene from 236 to 374 K. It is clear that the lower-frequency peak becomes more pronounced when the temperature decreases. These results show that the lower-frequency peak is less favorable entropically, consistent with our assigning it to the OD stretch of the intra−intermolecular hydrogen-bonded 2MPOD. Lower entropy is consistent with a complex vs a free 2MPOD and a free solvent molecule. The shoulder at ∼2610 cm^{-1} is the peak of the 2MPOD−toluene complex. The increasing amplitude of this peak with decreasing temperature shows that the equilibrium shifts to more complexes at lower temperatures.

Figure 4A and B are van't Hoff Plots[36] for 2MPOD in toluene plotted from 297 to 345 K and from 250 to 291 K (independent measurements). The enthalpy of formation of the 2MPOD/toluene complex in the toluene solution (or the intermolecular part of the intra−intermolecular hydrogen bonding) is −0.61 kcal/mol for both plots. (The concentration of the toluene in the solution is taken to be the standard concentration.) The energy of formation of the 2MP−toluene complex from DFT calculations is −0.5 kcal/mol (with zero-point energy correction). The entropy of formation is −12.1 and −11.1 J/(mol K) from Figure 4A and B, respectively. The population ratio (also the equilibrium constant, assuming the concentration of the toluene in the solution to be the standard concentration) of the complex to free 2MPOD in toluene at 297 K (room temperature) is 0.66.

The data discussed above clearly show that an equilibrium exists between two species, which have been taken to be the three-centered hydrogen-bonded 2MPOD−toluene complex in equilibrium with free 2MPOD. However, it is reasonable to consider other possibilities. In CCl_4 and other nonaromatic solvents such as hexane, only a single peak is observed in the IR spectrum (see Figure 2). Therefore, the two species in equilibrium must be associated with a complex to the aromatic solvent. A possibility other than the proposed three-centered hydrogen-bonded complex in equilibrium with the free intramolecular hydrogen-bonded 2MPOD is a two-centered complex in which the intramolecular hydrogen bond is broken and a pure intermolecular hydrogen bond between the hydroxyl and toluene is formed. Figure 5 shows FTIR spectra of 2MPOD and pMPOD in toluene. pMPOD does not have an intramolecular hydrogen bond. The smaller peak for pMPOD at 2668 cm^{-1} is for the free OD stretch. The main peak at 2630 cm^{-1} belongs to the intermolecular hydrogen-bonded OD stretch (the hydrogen bond acceptor is the toluene π-electron system). Intermolecular hydrogen bonding produces a red shift.[2,14] The magnitude of the shift is consistent with that observed for the phenol−benzene complex.[14] In the 2MPOD spectrum, the peak at ∼2625 cm^{-1} is the free 2MPOD hydroxyl stretch red shifted by the intramolecular hydrogen bond (the hydrogen bond acceptor is the electron pair of the oxygen of the methoxyl group; see Figure 2). Then, the additional red shifting of the peak at ∼2610 cm^{-1} is produced by additional intermolecular hydrogen bonding to form the three-centered complex. This peak has a larger red shift (more hydrogen bonding) than either the intermolecular or intramolecular hydrogen bonds by themselves. It is interesting to note that the 2MPOD pure intramolecular hydrogen bond OD stretch is at 2629 cm^{-1} (Figure 2), which is only 1 cm^{-1} different from that of the pure intermolecular hydrogen bond of pMPOD with toluene. The intramolecular hydrogen bond is a weak hydrogen bond because of the unfavorable geometry.[2] The fact that the two peaks have virtually the same frequency shows that the intermolecular bond of the hydroxyl to the aromatic ring is about the same strength as the weak intramolecular hydrogen bond. The fact that the two types of hydrogen bonds have about the same strength is a play off influences. Normally, hydrogen-bonding interactions would be stronger for an oxygen acceptor than for the π-electrons of toluene as the acceptor. However, the geometric constraint of the intramolecular hydrogen bond weakens the hydrogen bond. The unfavorable geometry of the intramolecular hydrogen bond reduces the efficacy associated with the oxygen acceptor compared to the intermolecular π-electrons as the acceptor, resulting in intra- and intermolecular hydrogen bonds of about the same strength.

For 2MPOD/toluene, the peak at 2625 cm^{-1} is assigned to an intramolecular hydrogen bond only, and the shoulder at 2610

(36) Chang, R. *Physical Chemistry for the Chemical and Biological Sciences*; University Science Books: Sausalito, 2000.

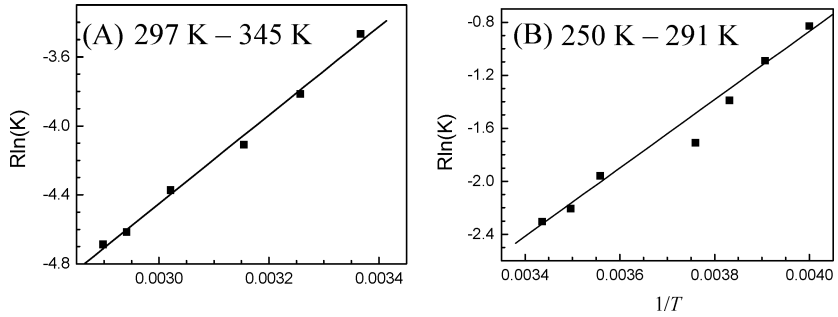

Figure 4. van't Hoff Plots derived from two sets of temperature-dependent FTIR measurements. The formation enthalpy for the intra−intermolecular hydrogen bond is found to be −0.6 kcal/mol from both measurements.

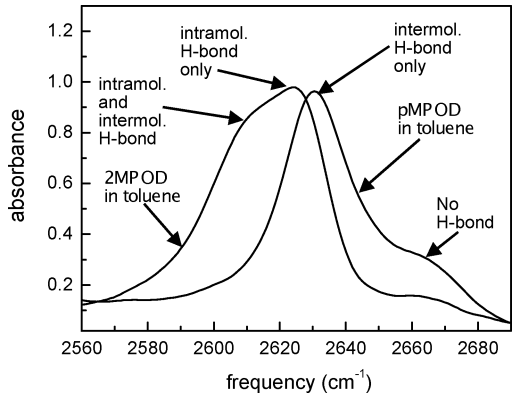

Figure 5. Hydroxyl stretch FTIR spectra of 2 wt % *p*-methoxyphenolOD (pMPOD) and 2-methoxyphenolOD (2MPOD) in toluene. The pMPOD spectrum shows two bands. The higher-frequency small shoulder is the free species, and the lower-frequency band is the intermolecular hydrogen-bonded complex. The 2MPOD spectrum shows two bands. The higher-frequency band is the free species with its intramolecular hydrogen bond, and the lower-frequency band is the intra−intermolecular hydrogen-bonded complex.

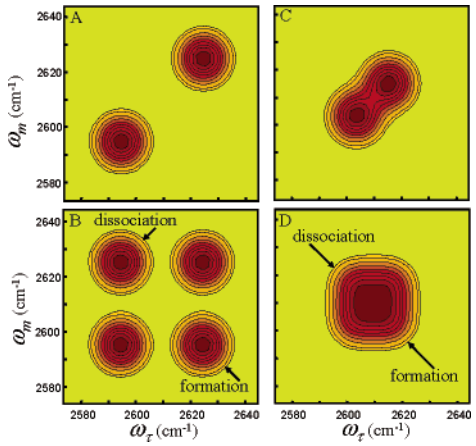

Figure 6. Schematic illustrations showing the peaks appearances at short and long T_w in 2D IR spectra for two peaks that are well resolved in the linear absorption spectrum (A before exchange and B after exchange) and for two overlapping peaks (C before exchange and D after exchange). The growth of the off-diagonal peaks will form a square rather than resolved off-diagonal peaks for two peaks that overlap substantially in the linear absorption spectrum.

cm^{-1} is assigned to the intra−intermolecular bond. The peak at 2625 cm^{-1} has almost the same position as the intermolecular hydrogen bond only peak for pMPOD/toluene (Figure 5) and the intramolecular hydrogen bond only peak for 2MPOD/CCl_4 (Figure 2). Another possibility is that the 2MPOD/toluene peak at 2625 cm^{-1} is the intermolecular hydrogen bond only, and the equilibrium with the intra−intermolecular bond (shoulder at 2610 cm^{-1}) involves making and breaking the intramolecular hydrogen bond rather than formation and dissociation of the solute−solvent complex. Although this seems implausible, it cannot in fact be ruled out by the linear spectroscopy alone. However, electronic structure calculations show that the activation energy to break the intramolecular hydrogen bond is >5 kcal/mol. This high barrier would produce slow exchange, estimated to be >100 ps. As shown below, the 2D IR results measure 3 ps, confirming the assignments given in Figure 5.

B. 2D IR Vibrational Echo Experiments and Analysis of the Dynamics. The dissociation enthalpy (negative sign of the formation enthalpy) of the intra−intermolecular hydrogen bonding was determined to be 0.6 kcal/mol, which is almost identical to the thermal energy at room temperature. Therefore, it might be anticipated that the 2MPOD−toluene complex dissociation time is fast. Recently, it has been demonstrated that 2D IR VES can be used to directly measure chemical exchange in real time under thermal equilibrium conditions.[13−15] In addition, 2D NMR has been used to measure chemical exchange on much slower time scales for some time,[37] although there are significant differences between 2D IR VES chemical exchange measurement on ultrafast time scales and 2D NMR measurements. Here, a qualitative discussion will be presented.

First, consider the case in which the linear IR spectrum shows well-resolved peaks for two species, e.g., a hydrogen-bonded complex and a nonbonded one (the phenol/benzene−CCl_4 system is of this type; see ref 14). The peak for the complex is at lower frequency. At T_w's that are short compared to the exchange time, the 2D IR vibrational echo spectrum will consist of two peaks on the diagonal, reflecting the 0−1 transitions of the two vibrations. This is shown schematically in Figure 6A. Again, the peak for the complex is at a lower frequency along the ω_m axis. Two other peaks (not shown), corresponding to the 1−2 transitions, will appear off diagonal, shifted to lower frequency along the ω_m axis by their vibrational anharmonicities.[14,38] These peaks have been discussed in detail in the context of 2D IR VES chemical exchange[14] and will be returned to when needed later. At T_w's that are long compared to the chemical exchange time (inverse of the rate constant of formation and dissociation of the complex), off-diagonal peaks will have grown in, which is shown schematically in Figure 6B. The peak labeled dissociation appears as the complex dissociates, and the peak labeled formation appears as the complex forms. The rate of growth of the off-diagonal peaks provides the chemical exchange

(37) Ernst, R. R.; Bodenhausen, G.; Wokaun, A. *Nuclear Magnetic Resonance in One and Two Dimensions*; Oxford University Press: Oxford, 1987.
(38) Rector, K. D.; Kwok, A. S.; Ferrante, C.; Tokmakoff, A.; Rella, C. W.; Fayer, M. D. *J. Chem. Phys.* **1997**, *106*, 10027.

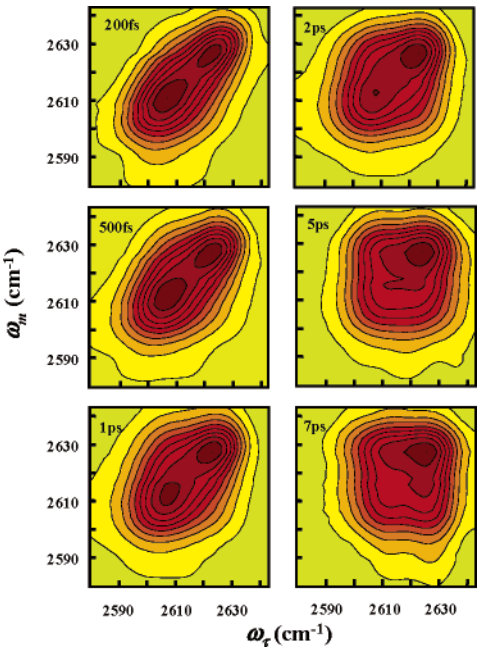

Figure 7. Shows the 0−1 region of the T_w dependent 2D vibrational echo spectrum for 2MPOD in toluene. The growth of the cross-peaks changes the shape of the spectrum, which becomes square after substantial exchange.

kinetics when properly analyzed. If the system is in equilibrium, the rate of formation equals the rate of dissociation, and the two off-diagonal peaks grow in together (see further discussion below).

For the situation in which the linear IR absorption of the complex appears as a shoulder on the low-frequency side of the free 2MPOD (see Figure 2), at a short T_w, the spectrum will appear as in Figure 6C. The peaks in the 2D spectrum appear on the diagonal but overlap in a manner related to the overlap in the linear spectrum. For T_w's that are long compared to the exchange time, off-diagonal peaks will have grown in. As with the diagonal peaks, the off-diagonal peaks will overlap the diagonal peaks, as illustrated schematically in Figure 6D. Although the off-diagonal peaks are not well resolved as they are in Figure 6B, they are clearly in evidence by the change in shape from the short time spectrum to an approximately square shape. It is straightforward to obtain the exchange rate by observing the growth of the off-diagonal peaks. As has been discussed in detail, whether the off-diagonal peaks are well resolved or not, to obtain the chemical exchange rate constant, it is necessary to fit all four peaks (diagonal and off-diagonal) in the 2D IR vibrational echo spectrum.

Figure 7 displays T_w-dependent 2D IR vibrational echo spectra of the 2MPOD−toluene system for the 0−1 transition region. For each panel, there are the equivalent peaks for the 1−2 transition region shifted to lower frequency along the ω_m axis by the 100 cm^{-1} anharmonicities of the transitions. These are not shown but were used in part of the data analysis as discussed below. Each contour represents a 10% change in amplitude of the peaks. The 200 fs panel corresponds to a short T_w at which negligible chemical exchange has occurred. In Figure 2, the complex appears as the low-energy shoulder on the 2MPOD in the toluene spectrum. In the 200 fs panel of Figure 7, the two peaks, the 2MPOD−toluene complex and free 2MPOD, are clearly visible on the diagonal. The complex and free peaks are the lower-frequency (2611 cm^{-1}) and higher-frequency (2629 cm^{-1}) peaks along the ω_m axis, respectively. Compared with the 1D IR spectrum in Figure 2, the 2D spectrum clearly resolves the two species better. In the 1D spectrum, the complex is a shoulder on the low-energy side of the free peak, and in the 2D spectrum, the two peaks are distinct. As with the 2MPOD−toluene spectrum in Figure 2, the hydroxyl stretch transition is shifted to lower frequency because of increased hydrogen bonding when the three-centered complex is formed. In the 500 fs panel, it is evident that the shape has begun to change, and in the 1 ps panel, the effect of the growth of the off-diagonal peaks on the shape of the spectrum is very clear. In the 2 ps spectrum, the shape is almost the approximately square shape discussed in connection with Figure 6, and the 5 ps spectrum has obtained the approximately square shape illustrated schematically in Figure 6D.

Other factors besides chemical exchange also influence the 2D spectrum. These are spectral diffusion,[39] orientational relaxation,[40] and vibrational relaxation.[41] None of these produce off-diagonal peaks. Spectral diffusion is the result of time-dependent interactions of the vibrational transition with the solvent. These interactions cause the transition frequency to fluctuate. At short time, the diagonal peaks' line shapes measured in the 2D vibrational echo spectrum are elongated along the diagonal, which is caused by inhomogeneous broadening. As T_w increases, the frequency of each molecule samples an increasing fraction of the entire absorption spectrum (spectral diffusion). At sufficiently long T_w, the entire line is sampled, and the dynamic line width is equal to the absorption line width. In the 2D spectrum, complete spectral diffusion is manifested by a change in the 2D line shape from elongated along the diagonal to symmetrical about the diagonal.[33] This change can be seen most clearly by comparing the central contours of the free peak at 200 fs and 2 ps.

Spectral diffusion changes the shapes of the peaks but preserves their volumes.[14,33] Orientational relaxation and vibrational relaxation cause all peaks to decay in volume in contrast to chemical exchange, which causes the off-diagonal peaks to grow and the diagonal peaks to shrink. Orientational relaxation during the T_w period reduces the peak volumes but does not cause them to decay to zero.[14,42] Vibrational relaxation does cause the peaks to eventually decay to zero. The relaxation times are not the same for the two species, which can be seen in the 2D spectra. Each spectrum has been normalized to the largest peak at the associated T_w. By comparing the 200 fs and 2 ps data, particularly the central contour, it is clear that the diagonal peak for the complex has decayed more rapidly than the diagonal peak for free 2MPOD.

All of the dynamical phenomena discussed qualitatively above are combined in the quantitative analysis of the data. The data are analyzed to obtain the formation and dissociation rates of the three-centered hydrogen-bonded complex using a combination of time-dependent diagrammatic perturbation theory, which describes the nonlinear optical interactions with the molecular vibrations,[33,43] and kinetic equations.[14] A brief discussion is presented here. Figure 8A,B qualitatively illustrates the radiation

(39) Tokmakoff, A.; Urdahl, R. S.; Zimdars, D.; Francis, R. S.; Kwok, S.; Fayer, M. D. *J. Chem. Phys.* **1995**, *102*, 3919−3931.
(40) Berne, B. J.; Pecora, R. *Dynamic Light Scattering*; J. Wiley: New York, 1976.
(41) Egorov, S. A.; Everitt, K. F.; Skinner, J. L. *J. Phys. Chem. A* **1999**, *103*, 9494−9499.
(42) Berne, B. J.; Pecora, R. *Dynamic Light Scattering*: J. Wiley: New York, 1990.

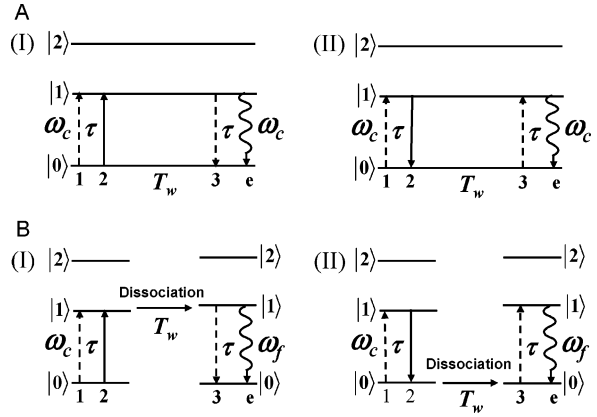

Figure 8. Energy level diagrams with radiation field interactions representing the pathways that give rise to the diagonal and off-diagonal peaks in Figure 7. See text.

field-matter interactions that give rise to the diagonal peak for the three-centered complex [$(\omega_\tau, \omega_m) = (2611\ \text{cm}, 2611\ \text{cm}^{-1})$] and the off-diagonal peak created by dissociation of the complex (2611, 2629 cm^{-1}) in the 0−1 region of the spectrum, respectively. The frequency of the complex is $\omega_c = 2611\ \text{cm}^{-1}$, and the frequency of free 2MPOD is $\omega_f = 2629\ \text{cm}^{-1}$. The other peaks in the 0−1 and 1−2 regions are obtained in the analogous manner. The frequency at which the first radiation field interaction (first pulse) excites a mode is the mode frequency on the ω_τ axis (horizontal axis) in the 2D spectrum. The first interaction produces a coherence (coherent superposition state) between the 0 and 1 states. In Figure 8, coherences are represented by dashed arrows. The second interaction with the radiation field (second pulse) produces a population (solid arrows) either in the 1 state (I in Figure 8) or in the 0 state (II in Figure 8). The third interaction (third pulse) again produces a 0−1 coherence followed by the vibrational echo emission (wavy arrow) at the same frequency as the coherence induced by the third pulse. The frequency of the vibrational echo emission is the frequency on the ω_m axis (the vertical axis). In Figure 8, the pathways I and II each contribute half of the signal.

First, consider Figure 8A for complexes that have not dissociated during the T_w period (or have dissociated and reformed a complex prior to the third pulse). Both pathways (I and II) begin at frequency ω_c and emit the vibrational echo at ω_c. Therefore, $\omega_\tau = \omega_m = \omega_c$, giving rise to the diagonal peak for the complex (2611, 2611 cm^{-1}). Now, consider Figure 8B for complexes that dissociate during the T_w period. The first interaction is at ω_c, but the last interaction and vibrational echo emission are at ω_f. Therefore, $\omega_\tau = \omega_c$ but $\omega_m = \omega_f$, giving rise to the off-diagonal peak for dissociation (2611, 2629 cm^{-1}). At short T_w (Figure 7, 200 fs; Figures 6A,C) only Figure 8A comes into play, and there are only peaks on the diagonal. At long T_w (Figure 7, 5 ps; Figure 6B,D) both 8A and B contribute to the signal, and there are diagonal and off-diagonal peaks.

The exchange during the τ period (time between pulses 1 and 2) is not considered here because for slow or moderate exchange rates it causes decay of the diagonal peaks but does not contribute to the off-diagonal peaks. If the exchange is much faster than the frequency difference between two peaks (18 cm^{-1} → 1.85 ps), motionally narrowing will result in a single peak in the spectrum.[44−46] In the systems considered here, the exchange rate is relatively slow.

(43) Mukamel, S. *Annu. Rev. Phys. Chem.* **2000**, *51*, 691−729.

Inspection of the data in Figure 7 shows that complexes form and dissociate on a few picoseconds time scale. Because of spectral diffusion, the shapes of the peaks change with T_w. In the absence of all other dynamical processes, the change in shape preserves the volume of a peak, but the peak amplitude is reduced as the peak broadens along the ω_τ axis. Therefore, the integrated peak volumes are fit to obtain the population dynamics. The volume of each peak as a function of T_w is obtained for each species by fitting the entire spectrum at each T_w with four 2D Gaussians. These fits can reproduce the spectrum at each T_w almost perfectly. The volumes are then scaled appropriately by the transition dipole moment ratio of the complexed and free species to obtain the population for each species. The populations are fit with the kinetic equations to yield the exchange rate constants. By using the peak volumes, spectral diffusion is accounted for.

As described above, there are three processes that contribute to the change in the peak volumes: the OD vibrational relaxation in free and complexed 2MPOD (lifetimes $T_f = 1/k_f$ and $T_c = 1/k_c$), the orientational relaxation (time constants $\tau_f = 1/(6D_f)$ and $\tau_c = 1/(6D_c)$; D_i is the orientational diffusion constant), and the chemical exchange dissociation and association rate constants k_d and k_a. The vibrational relaxation and orientational relaxation lead to diminishing intensities of all peaks with increasing T_w. Even complete orientational randomization during the T_w period does not cause the vibrational echo to decay to zero. Therefore, the chemical exchange time does not have to be short compared to the orientational relaxation time. The chemical exchange causes the diagonal peaks to diminish and the off-diagonal peaks to grow, as can be seen in Figure 7. On the basis of these considerations, a kinetic model was constructed.[14,47] The kinetic scheme is shown here for two peaks, the diagonal peak at 2611 and 2611 cm^{-1} (CC) and the off-diagonal peak at 2611 and 2629 cm^{-1} (CF) in Figure 7. CC represents the population of complexes at the end of the T_w period (the time of the third pulse) that were also complexes immediately after the second pulse. CF represents the population that were complexes immediately after the second pulse but are free 2MPODs at the end of the T_w period. Some complexes may have dissociated after the second pulse but reassociated by T_w. These are part of the CC population. It is also possible for a complex to dissociate, reassociate, and dissociate again during the T_w period. These would be part of the CF population and so forth. In this model, orientational relaxation is taken to be diffusive.[47] This is born by the fact that the measured time-dependent anisotropies decay exponentially. The model is illustrated schematically as:

$$\xleftarrow[\text{decay}]{\tau_c, T_c} \text{CC} \underset{k_a}{\overset{k_d}{\rightleftharpoons}} \text{CF} \xrightarrow[\text{decay}]{T_f, \tau_f}$$

The differential equations derived from this kinetic model are

$$\frac{d([\text{CC}(t)] \times f_c(t,\theta))}{dt} = -(k_c + k_d + D_c\text{I}^2) \times ([\text{CC}(t)] \times f_c(t,\theta)) + k_a \times ([\text{CF}(t)] \times f_f(t,\theta))$$

$$\frac{d([\text{CF}(t)] \times f_f(t,\theta))}{dt} = -(k_f + k_a + D_f\text{I}^2) \times ([\text{CF}(t)] \times f_f(t,\theta)) + k_d \times ([\text{CC}(t)] \times f_c(t,\theta)) \quad (1)$$

where the quantities in square brackets are the time-dependent concentrations, $f_i(t,\theta)$ is the angular distribution function for the complex (c) and the free species (f), I^2 is the spherical harmonic operator, D_c and D_f are the rotational diffusion constants, and k_c and k_f are the vibrational decay constants. k_a and k_d are the association and dissociation rate constants.[47] From these two equations, the equations for the time-dependent volumes of peak CC ($V_{CC}(t)$) and CF ($V_{CF}(t)$) are derived. The complete solutions of these equations are given in the Supporting Information. In the above equations, only k_a and k_d are unknown variables, and all the other parameters are experimentally measured. The dissociation rate (number per unit time) of the complex equals the formation rate if the system is in equilibrium. The complex dissociation time constant, τ_d (given in picoseconds below), is independent of concentration. Therefore, τ_d is reported and discussed. $\tau_d = 1/k_d$, where $k_d = k_a/0.66$ is the dissociation rate constant. The dissociation rate is k_d[complex]. Because the equilibrium constant is known, there is actually a single unknown parameter. The volumes are scaled appropriately by the transition dipole moment ratio for the two species. The volumes of the diagonal peaks, V_{CC} and V_{FF}, depend on the fourth power of their respective transition dipole moments, μ_c^4 and μ_f^4. The off-diagonal peaks, V_{CF} and V_{FC}, both depend on $\mu_c^2\mu_f^2$. μ_c and μ_f are the 0−1 transition dipole moments of the OD stretch for the complexed 2MPOD and free 2MPOD. It was determined experimentally that $\mu_c^2 = 2\mu_f^2$ by combining the 1D and 2D IR measurements as mentioned above. Thus, the scaled volume is the actual volume divided by 1 for the free peak, divided by 4 for the complexed peak, and divided by 2 for the cross-peaks. A set of equations equivalent to eq 1 applies for the free diagonal peak (FF) and the free associating to complex off-diagonal peak (FC).

The data for the 0−1 transition region consist of four time-dependent components: the two diagonal peaks (the three-centered complex and the free 2MPOD) and the two off-diagonal peaks (dissociation and formation of the complex during the T_w period). All four peaks can be reproduced with the single adjustable parameter, τ_d, by inputting the known constants and fitting the data with the kinetic equations. The input parameters used are $T_c = 5$ ps, $T_f = 6.2$ ps, $\tau_c = 6.6$ ps, $\tau_f = 4.0$ ps, and the ratio of the complexed and free 2MPOD concentrations, [complex]/[free] = 0.66. The intramolecular hydrogen-bonded (free) 2MPOD vibrational lifetime (T_f) was directly obtained by measuring that of 2EPOD in toluene, and the rotational relaxation time constant was measured for 2EPOD and scaled by the volume ratio of 2MP and 2EP ($\tau_f = 4.4 \times 0.9 = 4$ ps). For the intra−intermolecular hydrogen-bonded 2MPOD, the rotational relaxation time constant was directly obtained from measuring that of the pMPOD in toluene (they have virtually the same volumes). The vibrational lifetime of the 2MPOD−toluene complex was obtained by performing a pump−probe experiment at 2610 cm^{-1}, which is on the shoulder of the spectrum in Figure 2. A fit to the spectrum showed that this wavelength is virtually pure complex absorption. However, exchange will modify the measured lifetime. The observed pump−probe decay is 4.9 ps. The lifetime of the free 2MPOD is 6.2 ps. Exchange will cause the observed pump−probe decay for the complex to be slower than the true lifetime. However, the exchange rate determined below is not highly sensitive to the lifetime. We found that variation of the value of 4.9 ps by ±1 ps did not change the value of the exchange rate. Once the exchange rate was determined, we used its value, the lifetime of the free species, the observed pump−probe decay for the complex, and the appropriate pair of coupled differential equations to determine the true lifetime of the complex to be 4.6 ps. Because the vibrational and rotational parameters for the 2MPOD solution were not measured directly, we allowed each parameter to vary ±1 ps in fitting the data and used the results to determine the error bars for τ_d.

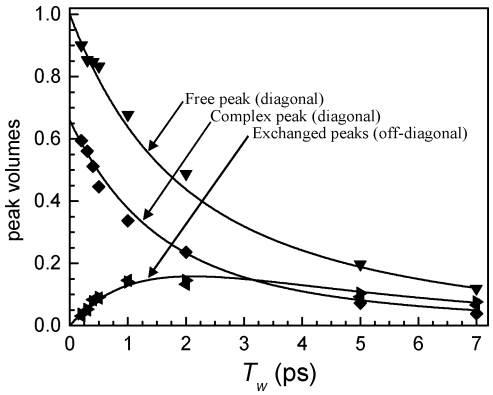

Figure 9. T_w dependent data (symbols) for 2MPOD showing the time dependence of the two diagonal and two off-diagonal peaks, in the 0−1 region of the 2D vibrational echo spectra as in Figure 7. The curves are from a fit to the data with one adjustable parameter, τ_d, using the kinetic model. Other parameters in the model are determined experimentally. $\tau_d = 3 \pm 0.6$ ps.

Figure 9 shows the peak volume data for the 0−1 transition region of the spectrum as a function of T_w. The data are normalized to the largest peak at $T_w = 0$. The simultaneous fit (solid curves) to the time dependence of all of the peaks using *a single adjustable parameter*, τ_d, is very good. From the fits, the dissociation time for the complex is $\tau_d = 3.0 \pm 0.6$ ps.

In addition to 2MPOD, pMMPOD was also studied in toluene. The data have the same appearance as those for 2MPOD (Figure 7). Figure 10A displays the peak volume data for the 0−1 transition region of the spectrum. The data were fit using the same data processing procedure described above. The input parameters are [complex]/[free] = 0.8, extinction coefficient ratio (complex/free) = 1.55, $T_c = 5$ ps, $T_f = 6.2$ ps, $\tau_c = 7.3$ ps, and $\tau_f = 4.4$ ps. The solid curves in Figure 10A are the results of the fits and yield $\tau_d = 3.4 \pm 0.6$ ps. The addition of a methyl in the para position may have a small influence on the complex dissociation time, but the difference falls within the error bars of the measurements.

The question arises as to whether τ_d's and the related formation and dissociation rates of the two systems studied here are in fact the dynamics under thermal equilibrium conditions. It is possible that the excitation of the hydroxyl stretch shifts the equilibrium, and the dynamics shown in Figures 9 and 10A in part reflect the relaxation to the new equilibrium concentrations. Two tests can be performed to determine if vibrational excitation has influenced the measurement of equilibrium dynamics. First, if the system is in thermal equilibrium, the two off-diagonal peaks will grow at the same rate because the rates of dissociation and formation are the same at equilibrium.[14] As

(44) Rollefso, R. J. *Phys. Rev. Lett.* **1972**, *29*, 410−412.
(45) Oxtoby, D. W. *J. Chem. Phys.* **1981**, *74*, 1503.
(46) Levinger, N. E.; Davis, P. H.; Behera, P.; Myers, D. J.; Stromberg, C.; Fayer, M. D. *J. Chem. Phys.* **2003**, *118*, 1312−11326.
(47) Cang, H. Thesis: Dynamics in Complex Liquids. Stanford University, Standford, CA, 2004.

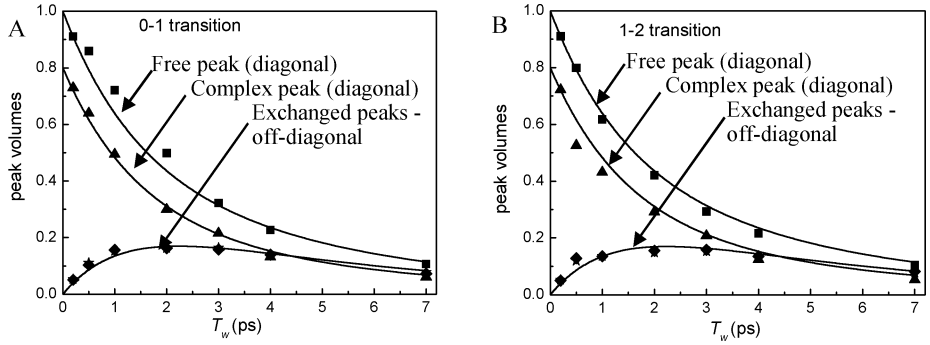

Figure 10. T_w dependent data (symbols) for pMMPOD in toluene showing the time dependence of the two diagonal and two off-diagonal peaks, in the 0−1 region (A) and the 1−2 region (B) of the 2D vibrational echo spectra. The curves in A are from a fit to the data with one adjustable parameter, τ_d, using the kinetic model. Other parameters in the model are determined experimentally. $\tau_d = 3.4 \pm 0.6$ ps. The curves in B are obtained without adjustable parameters using the same parameters as those in A. The agreement shows that the thermal equilibrium is not perturbed by vibrational excitation.

can be seen from Figures 9 and 10A, the growth of the formation and dissociation peaks (off-diagonal chemical exchange peaks) is identical within experimental error.

Another test involves comparing the 0−1 data to the equivalent data for the 1−2 transition. In Figure 8B, it can be seen that there are two pathways that contribute equally to the 0−1 signal. For one pathway, the system is in the ground state ($v = 0$) during the T_w period (Figure 8B(I)). For the other pathway, the system is in the excited state ($v = 1$) during the T_w period (Figure 8B(II)). Half, 50%, of the signal arises from each of these pathways. For the 1−2 portion of the 2D vibrational echo spectrum, there is one pathway that has the same first two interactions as those in Figure 8B(I). After the second interaction, the system is in the $v = 1$ state. The third interaction (third pulse) can produce a coherence between the $v = 1$ and $v = 2$ levels, and the vibrational echo is then emitted at the frequency of the 1−2 transition, which is shifted to lower frequency by the vibrational anharmonicity (100 cm^{-1}). The portion of the 2D spectrum that occurs from vibrational echo emission at the 1−2 frequency only involves a pathway in which the system is in the $v = 1$ state during the T_w period. Therefore, the 0−1 portion of the spectrum involves 50% of the signal in which the dynamics might be influenced by vibrational excitation whereas the 1−2 portion of the spectrum involves 100% of the signal that might be affected by vibrational excitation. If the measured dynamics are the same for these two portions of the spectrum, then vibrational excitation did not influence the thermal equilibrium chemical exchange rates.

2MPOD has an accidental degeneracy between the $v = 2$ level of the hydroxyl stretch and a combination band.[25] The accidental degeneracy results in additional overlapping peaks in the 1−2 portion of the spectrum which makes it difficult to analyze the time dependence of the chemical exchange. The addition of the *para*-methyl group in pMMPOD shifts the energies of the states sufficiently to eliminate the accidental degeneracy and clean 1−2 spectra results. Therefore, we performed the second test for perturbation of the thermal equilibrium dynamics on pMMPOD. Figure 10B shows the data for the 1−2 portion of the 2D spectrum. The curves through the data are not fits. They are calculated with no adjustable parameters using the parameters including τ_d obtained for the 0−1 transition. We find no difference in the kinetics for the 0−1 and 1−2 portions of the spectrum, within experimental error. Therefore, in these systems, vibrational excitation does not perturb the thermal equilibrium chemical exchange kinetics.

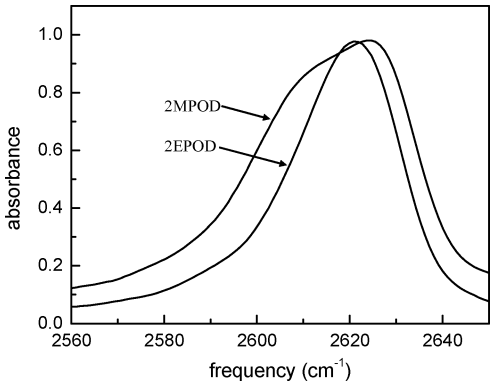

Figure 11. FTIR spectra of 2-methoxyphenolOD and 2-ethoxyphenolOD in toluene. The lack of a low-frequency shoulder in the 2EPOD spectrum shows there is little or no complex formation.

The same result was found for the phenol−benzene complex formation and dissociation.[14] It is important to point out that if vibrational excitation does perturb the chemical exchange kinetics of a system the ground-state thermal equilibrium kinetics can be recovered by using the observed kinetics from both the 0−1 and 1−2 portions of the spectrum in the analysis.

C. Structural Influences on the Intra−Intermolecular Hydrogen Bond. To explore some general chemical properties of the intra−intermolecular hydrogen bond, we varied the structures of both intramolecular and intermolecular acceptors and found that the three-centered hydrogen bond is very sensitive to small structural changes.

When one more methylene group is added to the methoxyl group of 2MPOD to become 2-ethoxyphenolOD (2EPOD), there is virtually no intermolecular hydrogen bonding between 2EPOD and toluene at room temperature, in contrast to 2MPOD. The difference between the two solutes' tendency to form complexes can be seen in the linear absorption spectrum shown in Figure 11. The 2EPOD spectrum has at most a very small shoulder on the low-frequency side in contrast to the 2MPOD spectrum. The shoulder in the 2MPOD spectrum arises from complex formation. 2D IR vibrational echo measurements confirmed the results from the linear IR spectra. Figure 12 shows 2D vibrational echo spectra for 2EPOD at $T_w = 200$ fs (A) and 2.5 ps (B). At 200 fs, there is a single peak elongated along the diagonal in contrast to the 200 fs panel of Figure 7. The elongation is caused by inhomogeneous broadening at short T_w. At 2.5 ps, the shape has changed substantially, becoming almost round, because of spectral diffusion. However, the characteristic approximately

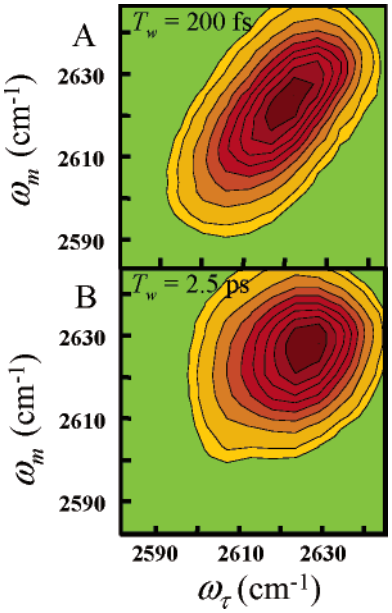

Figure 12. 2D IR spectra of 2-ethoxyphenolOD in toluene at (A) T_w = 200 fs and (B) T_w = 2.5 ps. A single peak appears in both spectra showing that no intra−intermolecular hydrogen-bonded complex is formed. The peak shape changes because of spectral diffusion.

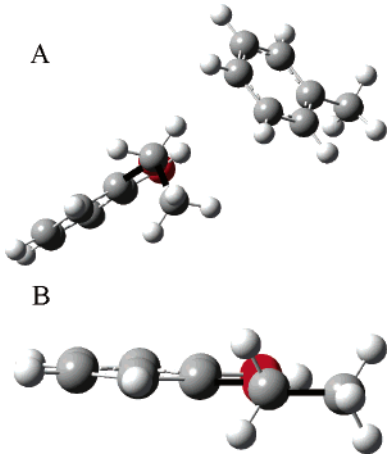

Figure 13. The structures of (A) the 2-ethoxyphenol/toluene complex and (B) 2-ethoxyphenol calculated with DFT at the B3LYP/6-31+G(d,p) level. See text.

square shape seen at the longer T_w's for 2MPOD (Figure 7) is absent. As discussed in conjunction with Figures 6 and 7, the square shape is indicative of the growth of off-diagonal peaks caused by chemical exchange between the complex and free species.

DFT structure calculations provide a possible explanation for the difference between 2EPOD and 2MPOD in their tendency to form a three-centered hydrogen bond with toluene. Figure 13A,B shows the optimized isolated molecule structures for the 2EP/toluene complex and the free 2EP molecule, respectively. To form the intra−intermolecular hydrogen bond with toluene, the end methyl group of 2EP has to be in the gauche position relative to the benzene ring. As can be seen in Figure 13A, the methyl group is below the plane of the benzene ring. If the ethyl substituent is in the anti configuration, the terminal methyl group prevents the toluene from obtaining the necessary position to form the intermolecular hydrogen bond. In contrast to the gauche configuration of 2EP necessary to form the three-centered complex, in the free 2EP, the methyl group is in the anti position relative to the benzene ring. The gauche configuration is ∼1.4 kcal/mol higher in energy than the anti configuration from the DFT calculations. It is important to emphasize that this calculation does not include toluene solvent. Thus, to form the intra−intermolecular hydrogen bond, 2EP must assume a higher energy configuration, which destabilizes the complex, compared to 2MP. The formation energy for the 2EP−toluene complex (isolated molecules, no solvent) is calculated to be 1.3 kcal/mol (with the zero-point energy correction), which is 1.8 kcal/mol higher than that of the 2MP/toluene complex (−0.5 kcal/mol from the equivalent calculation). On the basis of this energy difference, the Boltzmann distribution at room temperature gives the number of 2EP−toluene complexes to be <5% of the number of 2MP−toluene complexes. This is consistent with the lack of any obvious indication of 2EP−toluene complexes in either the absorption or 2D vibrational echo spectra.

The intra−intermolecular hydrogen bond is also formed between toluene and other ortho-substituted phenol derivatives, e.g., 2,6-dichlorophenol, 2-chlorophenol, and 2-bromophenol. In some sense, this intra−intermolecular hydrogen bond can also be called a π-hydrogen bond,[3] but it is different from the usual π-hydrogen bonds such as the bonding between phenol and benzene, in that the three-centered hydrogen bond is much more sensitive to steric effects on the benzene ring of the hydrogen bond acceptors. According to the literature[48,49] and our own results,[14] the binding energy between phenol and benzene (zero additional carbons on the ring), toluene (one additional carbon on the ring), *p*-xylene (two additional carbons on the ring), and mesitylene (three additional carbons on the ring) increases in the order of benzene < toluene < *p*-xylene < mesitylene because the π-electron density on the ring increases with increasing number of methyl substituents. The increase in the strength of the phenol complexes with an increased number of methyls on the acceptor occurs even though the steric effects that can inhibit the formation of the π-hydrogen bond increase with increased number of methyls. Therefore, in complexes with phenol, the π-electron density increase outweighs the adverse steric effects. The binding energies between 2MPOD and these aromatic solvents show the opposite trend, as demonstrated by the FTIR measurements displayed in Figure 14. In the linear IR spectra, the proportion of the shoulder at ∼2611 cm^{-1} for the intra−intermolecular hydrogen-bonded OD stretch clearly decreases as the number of methyl groups on the solvent increases. The strengths of the complexes are benzene > toluene > *p*-xylene > mesitylene. The results imply that the adverse steric effects that occur with an increased number of methyl groups are more important than the increases in π-electron density in forming the three-centered hydrogen bond in this series of solvents.

IV. Concluding Remarks

In this paper, the formation and dissociation of organic solute−solvent complexes were investigated. By performing temperature-dependent linear IR absorption experiments and 2D IR nonlinear vibrational echo measurements, it was determined

(48) Arnett, E. M.; Joris, L.; Mitchell, E.; Murty, T. S. S. R.; Gorrie, T. M.; Schleyer, P. v. R. *J. Am. Chem. Soc.* **1970**, *92*, 2365−2377.
(49) Fuchs, R.; Peacock, L. A.; Stephenson, W. K. *Can. J. Chem.* **1982**, *60*, 1953−1958.

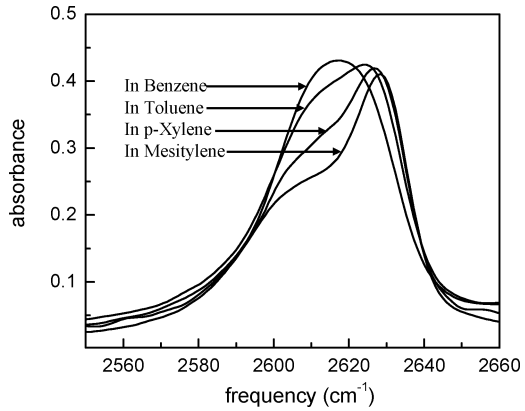

Figure 14. FTIR spectra of 2-methoxyphenolOD in benzene, toluene, *p*-xylene, and mesitylene. The intensity of the intra−intermolecular hydrogen-bonded complex peak decreases as more methyl groups are added to the benzene ring.

that the solute 2-methoxyphenol forms an unusual complex with the solvent toluene. The complex involves a three-centered hydrogen bond in which the 2MP hydroxyl hydrogen forms an intramolecular hydrogen bond with the methoxy oxygen and an intermolecular π-type hydrogen bond with the toluene. Both the thermodynamic and kinetic behaviors of the three-centered hydrogen bond were studied. The formation enthalpy of the 2MP−toluene complex was determined to be -0.6 ± 0.1 kcal/mol. 2D IR vibrational echo experiments showed that the formation and dissociation of the intra−intermolecular hydrogen-bonded complex happen on a picosecond time scale. The thermal equilibrium kinetics is characterized by the dissociation time, which was determined to be 3 ± 0.6 ps. It was experimentally demonstrated that the thermal equilibrium between the 2MPOD complex and free 2POD and intramolecular hydrogen-bonded 2MPOD and the exchange rates were not perturbed by the vibrational excitation on the hydroxyl stretch.

In addition to 2MP and toluene, several other related solutes and solvents were studied. It was found that the three-centered hydrogen bond is very sensitive to steric effects. The addition of a methylene group to the methoxyl group, that is, 2-ethoxyphenol (2EP), inhibits the formation of the intra−intermolecular hydrogen bond. DFT calculations show that the 2EP has to adopt a gauche conformation to be able to form the complex because complex formation is sterically prevented when 2EP is in the more stable anti conformation. The increased energy of the gauche conformation compared to the complex binding energy makes the 2EP−toluene complex improbable. It was also determined that the addition of methyl groups to the solvent molecules reduces the stability of the complex despite increased π-electron density in the solvent ring that would increase the strength of a conventional two-centered solute−solvent π-hydrogen bonding system, such as phenol−benzene.

Acknowledgment. We would like to thank Professor John I. Brauman for insightful discussions. This work was supported by a grant from AFOSR (F49620-01-1-0018) and from NSF (DMR-0332692).

Supporting Information Available: Analytical solutions for the kinetic model and 2D IR spectra including both 0−1 and 1−2 transitions. This material is available free of charge via the Internet at http://pubs.acs.org.

JA0570584